Study of measuring methods on spatial resolution of a GEM imaging detector*

LÜ Xin-Yu(吕新宇)[1,2;1)] FAN Rui-Rui(樊瑞睿)[1] CHEN Yuan-Bo(陈元柏)[1,3]
OUYANG Qun(欧阳群)[1,3] LIU Rong-Guang(刘荣光)[1,3] LIU Peng(刘鹏)[1]
QI Hui-Rong(祁辉荣)[1,3] ZHANG Jian(张健)[1,3] ZHAO Ping-Ping(赵平平)[1,3]
ZHAO Dong-Xu(赵东旭)[1] ZHAO Yu-Bin(赵豫斌)[1,3] ZHANG Hong-Yu(章红宇)[1,3]
SHENG Hua-Yi(盛华义)[1,3] DONG Li-Yuan(董丽媛)[4]

[1] Institute of High Energy Physics, Chinese Academy of Sciences, Beijing 100049, China
[2] Graduate University of Chinese Academy of Sciences, Beijing 100049, China
[3] State Key Laboratory of Particle Detection and Electronics, Beijing 100049, China
[4] School of Nuclear Science and Technology, Lanzhou University, Lanzhou 730000, China

Abstract: In this paper, the limitations of the common method measuring intrinsic spatial resolution of the GEM imaging detector are presented. Through theoretical analysis and experimental verification, we have improved the common method to avoid these limitations. Using these improved methods, a more precise measurement of intrinsic spatial resolutions are obtained.

Key words: spatial resolution, imaging detector, GEM, convolution, deconvolution

PACS: 29.40.Cs, 29.40.Gx, 29.90.+r **DOI:** 10.1088/1674-1137/36/3/007

1 Introduction

The GEM (Gas Electron Multiplier) is a typical Micro-Pattern gaseous detector, first invented in high energy physics, then applied in many other fields. We have constructed a 2-D imaging detector using triple-GEM for the BRSF (Beijing Synchrotron Radiation Facility) with an active area of 200 mm × 200 mm, which is able to detect X-rays with a high spatial resolution (Fig. 1). The GEM consists of a thin, metal-coated polymer foil, etched by a high density of holes. When a potential is applied between the electrodes up and down, radiation electrons drift into the holes, multiply and transfer to the other side. Each hole acts as an individual proportional amplifier. In our detector, three GEM foils are used to get a much higher gain.

One important specification of an imaging detector is the intrinsic spatial resolution (resolution will be used for short later in this paper). There are several definitions of resolution according to different criteria, however, all of them are equivalent in fact. Take FWHM and the standard deviation σ_0 for instance: when the consideration function is the normal distribution, the relationship between standard deviation σ_0 and FWHM is FWHM $= 2\sqrt{2\ln 2}\sigma_0$. In this paper, the standard deviation is chosen to be used as the resolution [1, 2]. Overall, resolution is to describe the resolving power of imaging detectors, so how to measure the resolution accurately is important.

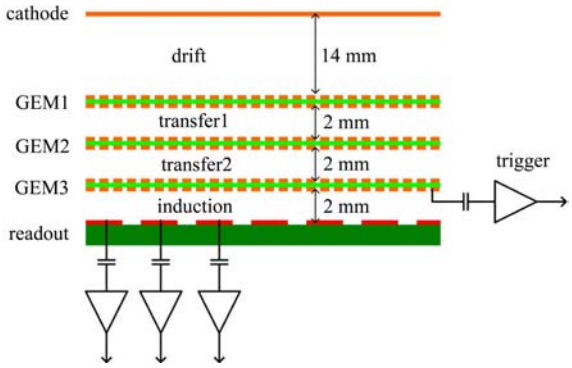

Fig. 1. The schematic view of our GEM detector structure.

Received 25 May 2011, Revised 14 July 2011
* Supported by Knowledge Innovation Program of Chinese Academy of Sciences
1) E-mail: lvxy@ihep.ac.cn

2 Analysis of the measurement of the spatial resolution of imaging detectors

2.1 The common method to measure spatial resolution

The common method to measure the resolution is usually to let beams be collimated by a slit (sometimes by a hole or a blade) (Fig. 2). The measurement result is always a distribution, of which standard deviation is σ. Then the resolution of the detector, of which standard deviation is σ_0, is obtained by Eq. (1).

$$\sigma_0 = \sqrt{\sigma^2 - h^2}, \tag{1}$$

where h is the width of the slit.

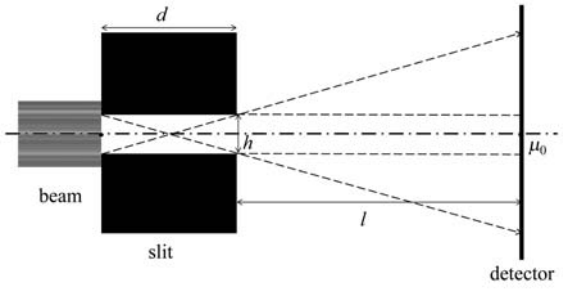

Fig. 2. The schematic view of beams collimated by a slit. The X-ray beams go through the collimator, which is horizontal. The detector surface is vertical.

We have carried out the measurement using this method in the condition: d=20 mm, h=0.2 mm, and l=40 mm. The σ of experimental data distribution is 1.33 mm. The resolution is calculated by Eq. (1).

$$\sigma_0 = \sqrt{1.33^2 - 0.2^2} = 1.3149 \text{ mm}. \tag{2}$$

Through a careful study, we have found limitations of this method and the error introduced in this method (Sec. 2.3).

2.2 Resolution of the detector, beam intensity distribution and experimental data distribution

When we use the GEM detector for X-ray imaging of an object, the beam (after going through the collimator) intensity on the surface of the detector is always a random variable, of which the distribution is called the beam intensity distribution. The distribution of data measured by the detector is called the experimental data distribution. Due to the electrons diffusion in the detector and the error existing in the measurement, the experimental data distribution cannot reflect the resolution function accurately. Experimental data distributions are often the result of the resolution function that is modified by the beam intensity distribution. In fact, the experimental data random variable Z is a superposition of the beam intensity random variable X and detector resolution random variable Y as shown in Eq. (3).

$$Z = X + Y. \tag{3}$$

According to the central limit theorem, the resolution function usually follows normal distribution. Hence, in the most general case, experimental data distributions are described by a convolution of a beam intensity distribution and the detector resolution function, where the p.d.f. (probability density function) of experimental data distributions is $g(x')$, that of beam intensity distribution $f(x)$ and that of resolution function $r(x'-x)$ (Eq. (4)).

$$g(x') = \int_{\Omega_x} r(x'-x) f(x) \mathrm{d}x, \tag{4}$$

Ω_x is the domain of the beam intensity random variable X. Its specific form is shown in Eq. (5) and Eq. (6).

Hence, the resolution can be calculated by fitting the experimental data distribution with $g(x')$ (Sec.3.1) or calculating $r(x'-x)$ by deconvolution (Sec. 3.2).

2.3 Limitations of the common method

With different beam intensity distributions, different experimental data distributions are obtained accordingly, as shown in Table 1. From the table, only when the beam intensity distribution and the detector resolution function both follow the normal distribution, can the resolution be calculated by Eq. (1). In many situations the beam intensity distribution does not follow normal distribution. In these conditions, if the width of the slit is smaller than one-tenth of the resolution (FWHM), the common method is still applicable according to GB/T 18989-200[1)]. This is the scope of application of the common method. To avoid this limitation, methods are improved to get a more precise resolution. Experiments with GEM detectors [3, 4] have been done to confirm these improved methods (Sec. 3).

1) Radionuclide imaging device performance and test rules for gamma camera

Table 1. Experimental data distributions as a convolution of resolution function and different beam intensity distributions.

p.d.f. of resolution function	p.d.f. of beam intensity distribution	p.d.f. of experimental data distribution
$\frac{1}{\sqrt{2\pi}\sigma_0}\mathrm{e}^{-\frac{(x'-x)^2}{2{\sigma_0}^2}}$	$f(x)=\delta(x-x_0)$ (extremely narrow slit)	$g(x')=\frac{1}{\sqrt{2\pi}\sigma_0}\mathrm{e}^{-\frac{(x'-x_0)^2}{2{\sigma_0}^2}}$
$\frac{1}{\sqrt{2\pi}\sigma_0}\mathrm{e}^{-\frac{(x'-x)^2}{2{\sigma_0}^2}}$	$f(x)=\frac{1}{b-a}$ (uniform distribution: a,b is the lower and upper limit)	$g(x')=\frac{1}{b-a}\left(F\left(\frac{b-x'}{\sigma_0}\right)-F\left(\frac{a-x'}{\sigma_0}\right)\right)*$
$\frac{1}{\sqrt{2\pi}\sigma_0}\mathrm{e}^{-\frac{(x'-x)^2}{2{\sigma_0}^2}}$	$f(x)=\frac{1}{\sqrt{2\pi}h}\mathrm{e}^{-\frac{(x-x_0)^2}{2h^2}}$ (normal distrubution)	$g(x')=\frac{1}{\sqrt{2\pi(h^2+{\sigma_0}^2)}}\mathrm{e}^{-\frac{(x'-x_0)^2}{2(h^2+{\sigma_0}^2)}}$

$*F(x)$ is cumulative distribution function of $f(x)$.

3 Improved methods to measure the spatial resolution of imaging detectors

3.1 Improved method 1: using a slit as the collimator with a convolution fit

As shown in Fig. 2, the surface of the detector, which is d+l away from the beam source, is perpendicular to the beam line. So Fig. 2 actually shows the one dimensional projection of the measurement frame. The beam source is a narrow strip source limited by the slit with a definite emission angle associated with the total domain Ω_x in Eq. (4). The total effect is that the intensity along the X-axis on the surface of the detector is proportional to the range of the source from where the X-ray beam can reach the surface. Due to the effect of the collimator, the beam intensity distribution is divided into three parts. P.d.f. of the beam intensity distribution is as shown in Eq. (5).

$$f(x)=\alpha\cdot\begin{cases}h-\dfrac{d}{l}\left(x-\mu_0-\dfrac{h}{2}\right) & x\in\left[\dfrac{h}{2}+\mu_0,\left(\dfrac{h}{2}+h\dfrac{l}{d}\right)+\mu_0\right]\\ h & x\in\left(-\dfrac{h}{2}+\mu_0,\dfrac{h}{2}+\mu_0\right)\\ h+\dfrac{d}{l}\left(x-\mu_0+\dfrac{h}{2}\right) & x\in\left[-\left(\dfrac{h}{2}+h\dfrac{l}{d}\right)+\mu_0,-\dfrac{h}{2}+\mu_0\right]\end{cases}\tag{5}$$

where μ_0 is the coordinate of the middle of the slit. $f(x)$ should be normalized.

$$\int_{-\left(\frac{h}{2}+h\frac{l}{d}\right)+\mu_0}^{\left(\frac{h}{2}+h\frac{l}{d}\right)+\mu_0}f(x)\mathrm{d}x=\alpha\cdot\left(\int_{\frac{h}{2}+\mu_0}^{(\frac{h}{2}+h\frac{l}{d})+\mu_0}\left[h-\frac{d}{l}\left(x-\mu_0-\frac{h}{2}\right)\right]\mathrm{d}x+\int_{-\frac{h}{2}+\mu_0}^{\frac{h}{2}+\mu_0}h\mathrm{d}x\right.$$
$$\left.+\int_{-\left(\frac{h}{2}+h\frac{l}{d}\right)+\mu_0}^{-\frac{h}{2}+\mu_0}\left[h+\frac{d}{l}\left(x-\mu_0+\frac{h}{2}\right)\right]\mathrm{d}x\right)=1.\tag{6}$$

From Eq. (6), we can get the normalization coefficient.

$$\alpha=1/h^2\left(\frac{l}{d}+1\right).\tag{7}$$

It is worth reminding ourselves that without the slit, the emission angle of the line source is 2π.

The curve of the beam intensity distribution, a solid black line in the shape of a trapezoid (like a dam), is shown in Fig. 3. When σ_0 is very small, the experimental data distribution is close to the beam intensity distribution (dashed line in Fig. 3). Otherwise, when σ_0 is very large, the experimental data distribution does not reflect the beam intensity distribution but just reflects the detector resolution function $r(x'-x)$ itself (dash-dotted line in Fig. 3).

In other words, if the detector resolution is much

larger than the slit width h, $g(x')$ is effectively approximated by $r(x'-x)$ and the collimator effect can be ignored, so an extremely narrow slit can be used as a collimator to verify these improved methods (Sec. 4).

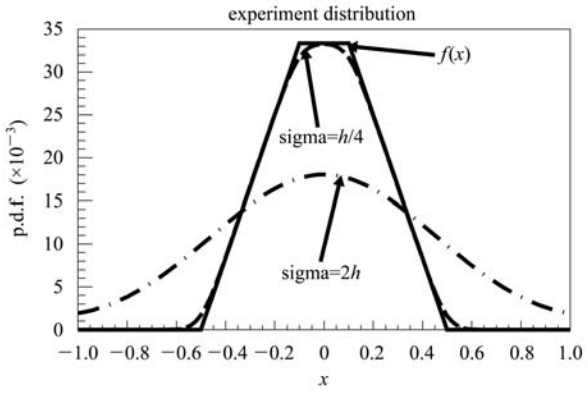

Fig. 3. Simulation study: the experimental data distributions as a function of the same collimator but different resolution of the detector.

Attention should be paid to one more affecting factor of oblique incidence shown in Fig. 4. Because of the incident angle $\angle\theta$, the quantity of the electrons on the top of GEM1 follows the uniformity distribution over the domain of $a\tan\theta$ (a is the space of the drift area of the GEM detector) instead of a point. So, all of the measurement results of resolution in this paper should remove the incident angle effect by subtracting $a\tan\theta$.

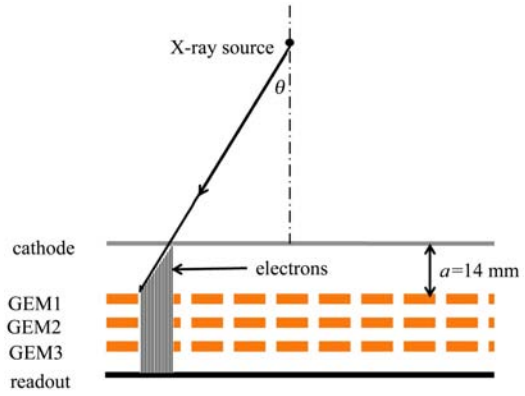

Fig. 4. The schematic view of the incident angle effect.

In this method, the beam intensity distribution is known, the resolution function follows the normal distribution, of which the standard deviation σ_0 can be treated as an undetermined coefficient. When we measure the resolution in experiments, the convolution function (Eq. (8)) is used to fit the experimental data distribution [5] to obtain the resolution of the detector. The measurement result on the GEM detector using this method is determined to be $\sigma_0 = 65.0$ μm.

$$g(x') = \alpha \cdot \begin{cases} \displaystyle\int_{\frac{h}{2}+\mu_0}^{\left(\frac{h}{2}+h\frac{l}{d}\right)+\mu_0} \frac{1}{\sqrt{2\pi}\sigma_0} \mathrm{e}^{-\frac{(x'-x)^2}{2{\sigma_0}^2}} \cdot \left[h - \frac{d}{l}\left(x-\mu_0-\frac{h}{2}\right)\right] \mathrm{d}x & x \in \left[\frac{h}{2}+\mu_0, \left(\frac{h}{2}+h\frac{l}{d}\right)+\mu_0\right] \\ \displaystyle\int_{-\frac{h}{2}+\mu_0}^{\frac{h}{2}+\mu_0} \frac{1}{\sqrt{2\pi}\sigma_0} \mathrm{e}^{-\frac{(x'-x)^2}{2{\sigma_0}^2}} \cdot h \ \mathrm{d}x & x \in \left(-\frac{h}{2}+\mu_0, \frac{h}{2}+\mu_0\right) \\ \displaystyle\int_{-\left(\frac{h}{2}+h\frac{l}{d}\right)+\mu_0}^{-\frac{h}{2}+\mu_0} \frac{1}{\sqrt{2\pi}\sigma_0} \mathrm{e}^{-\frac{(x'-x)^2}{2{\sigma_0}^2}} \cdot \left[h + \frac{d}{l}\left(x-\mu_0+\frac{h}{2}\right)\right] \mathrm{d}x & x \in \left[-\left(\frac{h}{2}+h\frac{l}{d}\right)+\mu_0, -\frac{h}{2}+\mu_0\right] \end{cases} . \quad (8)$$

The normalization coefficient $\alpha = 1/h^2\left(\frac{l}{d}+1\right)$

3.2 Improved method 2: using a blade as the collimator with deconvolution and convolution fit

In a 2-D image obtained from an imaging detector, it is reasonable that the sharper the image edge, the more precipitous its projection histogram. As shown in Fig. 5, the beam intensity distribution of the edge is a step distribution if a blade is used to

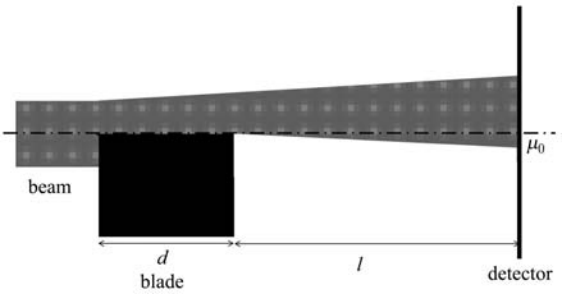

Fig. 5. The schematic view of using a blade as the collimator. d=2 cm, l=4 cm.

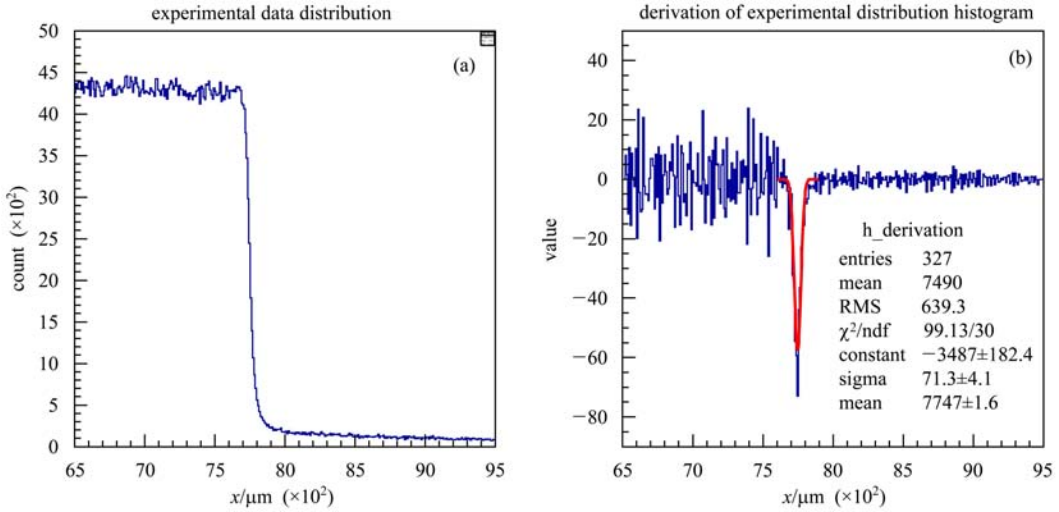

Fig. 6. Measurement result. (a) is the experimental data distribution; (b) is the derivation of the experimental data distribution.

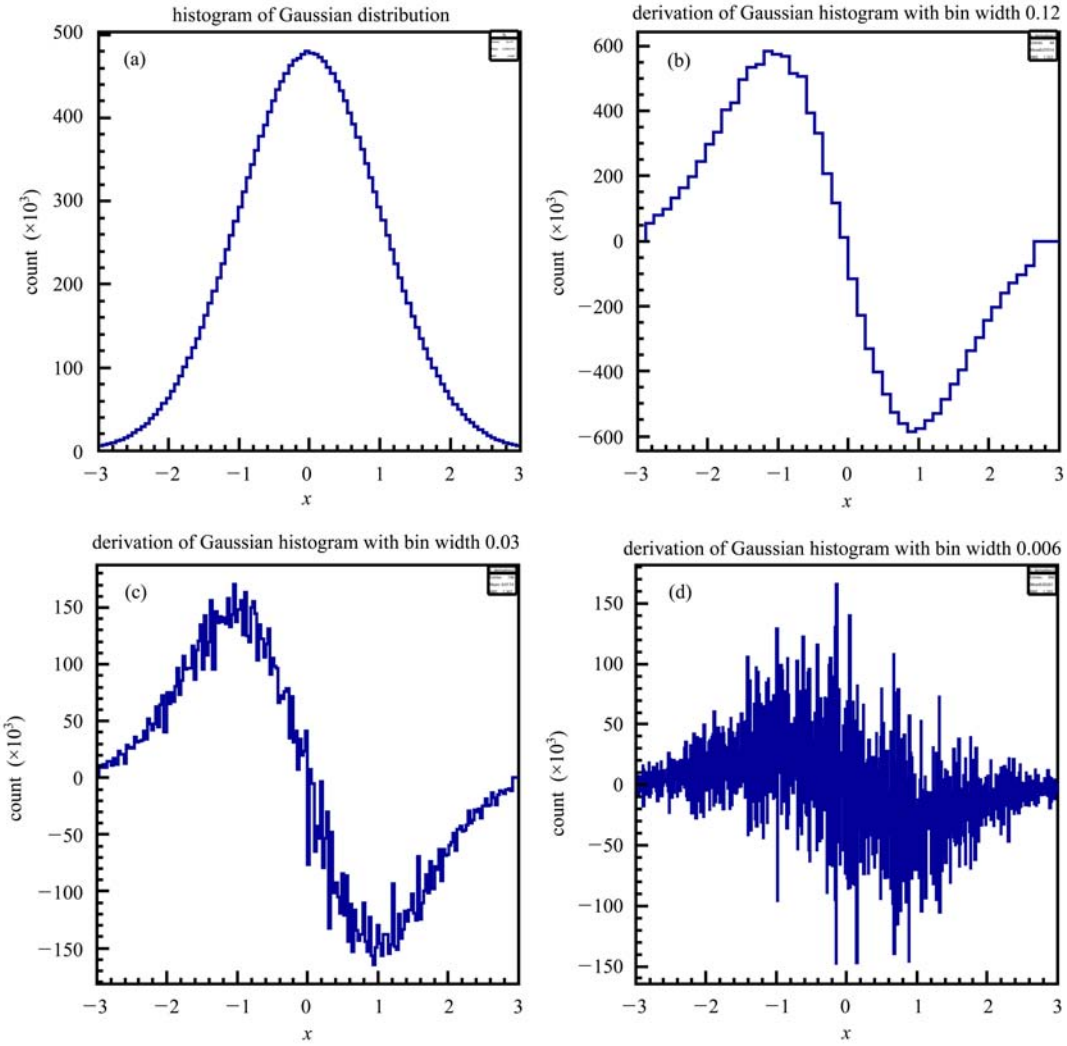

Fig. 7. Limited statistics in a bin of a histogram for a Gaussian distribution will yield different derivation distributions. (a) is a Gaussian distribution; (b), (c), (d) are derivations of the Gaussian distribution with different bin-widths.

cut the beam. The beam intensity above the blade nearly follows the uniform distribution. The beam intensity below the blade is zero. As the resolution function is a Gaussian distribution, the experimental distribution is a superposition of the step distribution and a Gaussian distribution, which is in fact the cumulative Gaussian distribution [6].

$$g(x') = \int_{x_{\min}}^{x'} r(t)\mathrm{d}t \tag{9}$$

The resolution function can be obtained by derivation of x on Eq. (9). σ_0 of the cumulative Gaussian distribution is the resolution. The process of solving the derivation (gradient) is that of deconvolution too. The measurement frame on the GEM detector using this method is shown in Fig. 5 and the result is $\sigma_0 = 71.3$ μm (Fig. 6). It is a little larger than the result of the first improved method, because the beam lines are not absolutely parallel.

It is worth noting that this method requires large statistics, otherwise, if there are insufficient statistics per bin, taking the Gaussian distribution as an example, the derivation distribution of the same Gaussian p.d.f for different bin widths will be different, as shown in Fig. 7; which yield different σ_0 for a Gaussian p.d.f. In our case, the total statistic is 2×10^6, while the bin width is 10 μm.

To avoid these drawbacks, we improved this method, the measurement architecture of which is the same as the deconvolution method but with different data processing. As described above, the edge of an image follows a cumulative Gaussian distribution. Indeed, the standard deviation of this Gaussian distribution is the resolution σ_0. So the cumulative Gaussian distribution with σ_0 as the undetermined coefficient can be used to fit the experimental data distribution. In this way, the resolution is determined to be $\sigma_0 = 63.3$ μm (Fig. 8).

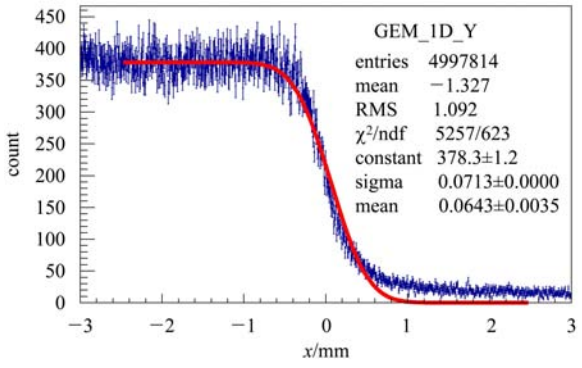

Fig. 8. The experimental distribution using a blade as the collimator.

4 Verification of the improved methods by using a extremely narrow slit as the collimator

As mentioned in Sec. 2.3, if the width of the collimator is narrow enough, less than one-tenth of the resolution (FWHM), the common method is applicable. In this method, an extremely narrow slit is used as the collimator. The measurement architecture is shown in Fig. 2, where h=0.01 mm, l=40 mm and d=20 mm. Because the slit is so narrow it allows very little of a beam to go through. High-intensity beams are required to get sufficient statistics. It is almost impossible to use the X-ray tube as the beam source in this situation. The measurement has been done at the BSRF, which can provide enough high intensity beams.

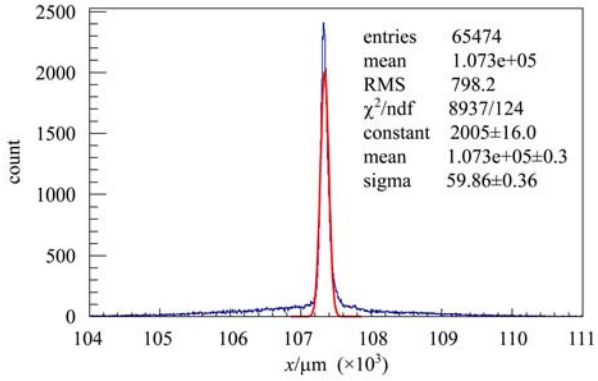

Fig. 9. The measurement result using an extremely narrow slit as the collimator.

The result is shown in Fig. 9. In this way, the resolution is $\sigma_0 = 59.9$ μm. The result is in line with those of the improved methods.

5 Measurement using the Rayleigh criterion

The Rayleigh criterion is the generally accepted criterion for the minimum resolvable detail when the first diffraction minimum of the image of one source point coincides with the maximum of another. That is to say, the intensity of the saddle between two peaks of the points is 81% of the intensity of each peak [7].

To use the Rayleigh criterion, we have measured the distribution using a collimator, which has 3 slits that are 0.32 mm in pitch. Each slit is 0.20 mm wide. The measurement result is shown in Fig. 10. As the width of each slit can not be ignored, the minimum

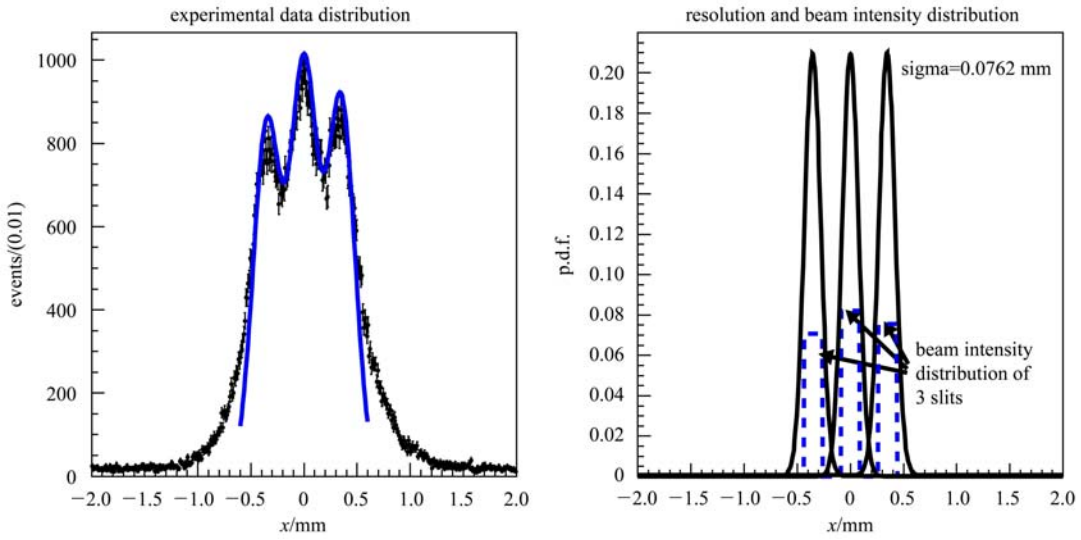

Fig. 10. The measurement result using the collimator with 3 slits. Left: the measurement data distribution. Right: the beam intensity distribution and the resolution function.

resolvable pitch is 0.32 mm (Fig. 10 left). After removing the effects of the width of each slit by a deconvolution fit, the resolution is $\sigma_0 = 76.2$ μm. It is a little larger than the results of the first and second improved methods mentioned above. That is because of the definition of the Rayleigh criterion. If the considered function is the normal distribution, according to the Rayleigh criterion, when the intensity of the saddle between two peaks of the points is 81% of the intensity of each peak, the distance center to center of the two peaks is $2.69\sigma_0$. Yet, the distance of the first and second improved methods is the FWHM, which is $2.355\sigma_0$. So the resolution using the Rayleigh criterion is $1.142\left(1.142=\dfrac{2.690}{2.355}\right)$ times larger than those of the first and second improved methods.

6 Summary and conclusion

The imaging detector's resolution can be limited by diffraction causing blurring of the image. By careful study of the relationship between the spatial resolution and the collimator, we give the scope of application of the common method and improve the method. The measurement using the improved method gives a more precise spatial resolution. Experimental validation has been done on the GEM detector as shown in Table 2.

Table 2. Summary of results of the measuring methods.

method#	σ_0 with incident angle correction/μm
common method	1314.9
method 1	65.0
method 2–1	71.3
method 2–2	63.3
extremely narrow slit	59.9
using the Rayleigh criterion	66.7*

$*66.7 = 76.2/1.142$.

The measurement is an exploration of the measurement of spatial resolution and a general reference to that of other imaging detectors. Further study taking more factors in to account is in progress.

References

1 XIE Y G, CHEN C et al. Particle Detector and Data Acquisition. Beijing: Science Press, 2003. 95–104 (in Chinese)
2 Tommaso Lari. Nucl. Instrum. Methods A, 2001, **465**: 112–114
3 DONG J, XIE Y G, CHEN Y B et al. HEP & NP, 2007, **31**(7): 664–668 (in Chinese)
4 LIU B, DONG J, LU X Y et al. Acta Physica Sinica, 2010, **59**: 6029–6035
5 Verkerke W, Kirkby D. RooFit Users Manual v2.91, 2008.
6 ZHU Y S. Probability and Statistics in Experimental Physics. Beijing: Science Press, Version 2, 2006. 47–51, 148–158 (in Chinese)
7 YAO Q J. Optics Tutorial. Beijing: Higher Education Press, Version 3, 2002. 287–290 (in Chinese)